Article

Three-Dimensional Self-Organization of Supramolecular Self-Assembled Porphyrin Hollow Hexagonal Nanoprisms

Jin-Song Hu, Guo, Han-Pu Liang, Li-Jun Wan, and Li Jiang

J. Am. Chem. Soc., **2005**, 127 (48), 17090-17095• DOI: 10.1021/ja0553912 • Publication Date (Web): 11 November 2005

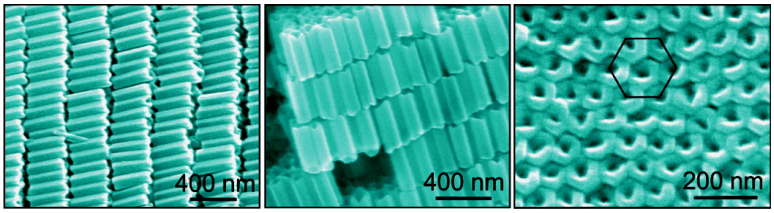

More About This Article

Additional resources and features associated with this article are available within the HTML version:

- Supporting Information
- Links to the 36 articles that cite this article, as of the time of this article download
- Access to high resolution figures
- Links to articles and content related to this article
- Copyright permission to reproduce figures and/or text from this article

View the Full Text HTML

J|A|C|S
ARTICLES
Published on Web 11/11/2005

Three-Dimensional Self-Organization of Supramolecular Self-Assembled Porphyrin Hollow Hexagonal Nanoprisms

Jin-Song Hu, Yu-Guo Guo, Han-Pu Liang, Li-Jun Wan,* and Li Jiang†

Contribution from the Institute of Chemistry, Chinese Academy of Sciences, Beijing 100080, China, and Schlumberger-Doll Research, Ridgefield, Connecticut 06877

Received August 17, 2005; E-mail: wanlijun@iccas.ac.cn

Abstract: A self-assembly technique assisted with surfactant is developed to fabricate one-dimensional (1D) nanostructure of zinc meso-tetra (4-pyridyl) porphyrin. The so-prepared nanostructure appears in a shape of hollow hexagonal nanoprism with uniform size. The length and aspect ratio of the nanoprisms is easily tunable by controlling the stoichiometric ratio of porphyrin over surfactant. The internal structure of the nanoprisms is well described by XRD. Furthermore, as a result of dispersivity and regular geometric shape, these nanoprisms can readily self-organize into an ordered, smectic three-dimensional (3D) architecture through simple evaporation of the solvent. The results should be significant in porphyrin crystallization and porphyrin application in optoelectronic device, catalysis, drug delivery, and molecular filtration.

Introduction

Self-assembly and self-organization are natural and spontaneous processes occurring mainly through noncovalent interactions such as van der Waals, hydrogen bonding, hydrophilic/hydrophobic, electrostatic, donor and acceptor, and metal−ligand coordination networks.[1] As a "bottom-up" strategy, self-assembly and self-organization are showing ever increasing importance in chemistry, material science, life science, and nanotechnology. As a result of understanding and fabricating living and natural systems from nonliving and artificial self-assemblies, a wide variety of nanometer or micrometer scale structures and assemblies has been generated, including micelles,[2] vesicles,[3,4] ribbons,[5−8] films,[9] fibers,[10,11] tubes,[12,13] wires,[14] and zeolites.[15] These organizations from molecular self-assemblies to controllable architectures and materials with advanced functions may meet the requirement of many objectives in science and technology such as sensor, electronic, and electromechanical device.[16−22]

Porphyrin, a family of macrocyclic organic molecules, has been extensively investigated in vastly diverse areas ranging from chemistry, physics, biology, and medicine to molecular device.[23] Such immense interests are stemmed from the biocompatibility of porphyrin and its ability to convert light energy into electron motion, as does its chlorophyll counterpart in light-harvesting complex upon which all the life forms on this planet depend. Among the investigations, one focus is the fabrication and preparation of designable assembly and nanomaterial.[24−31] It is well-known that the property of a nanostructured material or self-asembly will strongly depend on its morphology. Recently, Smith et al. reported that porphyrin nanorods several nanometers wide exhibit remarkable photoconductivity with a rapid turn on/off rate.[32] A composite porphyrin nanotube was produced by electrostatic force between two oppositely charged porphyrins.[33,34] These results are important achievements in the

† Schlumberger-Doll Research.

(1) Whitesides, G. M.; Grzybowski, B. *Science* **2002**, *295*, 2418.
(2) Zhang, L. F.; Yu, K.; Eisenberg, A. *Science* **1996**, *272*, 1777.
(3) Discher, D. E.; Eisenberg, A. *Science* **2002**, *297*, 967.
(4) Discher, B. M.; Won, Y. Y.; Ege, D. S.; Lee, J. C. M.; Bates, F. S.; Discher, D. E.; Hammer, D. A. *Science* **1999**, *284*, 1143.
(5) Gao, P. X.; Ding, Y.; Mai, W.; Hughes, W. L.; Lao, C. S.; Wang, Z. L. *Science* **2005**, *309*, 1700.
(6) Kong, X. Y.; Ding, Y.; Yang, R. S.; Wang, Z. L. *Science* **2004**, *303*, 1348.
(7) Oda, R.; Huc, I.; Schmutz, M.; Candau, S. J.; Mackintosh, F. C. *Nature* **1999**, *399*, 566.
(8) Wong, G. C. L.; Tang, J. X.; Lin, A.; Li, Y. L.; Janmey, P. A.; Safinya, C. R. *Science* **2000**, *288*, 2035.
(9) Stupp, S. I.; LeBonheur, V.; Walker, K.; Li, L. S.; Huggins, K. E.; Keser, M.; Amstutz, A *Science* **1997**, *276*, 384.
(10) Hartgerink, J. D.; Beniash, E.; Stupp, S. I. *Science* **2001**, *294*, 1684.
(11) Kato, T. *Science* **2002**, *295*, 2414.
(12) Yan, D. Y.; Zhou, Y. F.; Hou, J. *Science* **2004**, *303*, 65.
(13) Shimizu, T.; Masuda, M.; Minamikawa, H. *Chem. Rev.* **2005**, *105*, 1401.
(14) Li, Y. L.; et al. *J. Am. Chem. Soc.* **2005**, *127*, 1120.
(15) Kosal, M. E.; Chou, J.-H.; Wilson, S. R.; Suslick, K. S. *Nat. Mater.* **2002**, *1*, 118.
(16) Drain, C. M. *Proc. Natl. Acad. Sci. U.S.A.* **2002**, *99*, 5178.
(17) Du, C.; Falini, G.; Fermani, S.; Abbott, C.; Moradian-Oldak, J. *Science* **2005**, *307*, 1450.
(18) Kurth, D. G.; Lehmann, P.; Schütte, M. *Proc. Natl. Acad. Sci. U.S.A.* **2000**, *97*, 5704.
(19) Park, S.; Lim, J.-H.; Chung, S.-W.; Mirkin, C. A. *Science* **2004**, *303*, 348.
(20) Winfree, E.; Liu, F.; Wenzler, L. A.; Seeman, N. C. *Nature* **1998**, *394*, 539.
(21) Vriezema, D. M.; Aragones, M. C.; Elemans, J. A. A. W.; Cornelissen, J. J. L. M.; Rowan, A. E.; Nolte, R. J. M. *Chem. Rev.* **2005**, *105*, 1445.
(22) Cölfen, H.; Mann, S. *Angew. Chem., Int. Ed.* **2003**, *42*, 2350.
(23) *The Porphyrin Handbook*; Kadish, K., Smith, K. M., Guilard, R., Eds.; Academic Press: New York, 1999.
(24) Abrahams, B. F.; Hoskins, B. F.; Michail, D. M.; Robson, R. *Nature* **1994**, *369*, 727.
(25) Kim, D.; Osuka, A. *Acc. Chem. Res*. **2004**, *37*, 735.
(26) Takahashi, R.; Kobuke, Y. *J. Am. Chem. Soc.* **2003**, *125*, 2372.
(27) Stang, P. J.; Olenyuk, B. *Acc. Chem. Res.* **1997**, *30*, 502.
(28) Imamura, T.; Fukushima, K. *Coord. Chem. Rev.* **2000**, *198*, 133.
(29) Wojaczyński, J.; Latos-Grazyński, L. *Coord. Chem. Rev.* **2000**, *204*, 113.
(30) Lensen, M. C.; Takazawa, K.; Elemans, J. A. A. W.; Jeukens, C. R. L. P. N.; Christianen, P. C. M.; Maan, J. C.; Rowan, A. E.; Nolte, R. I. M. *Chem. Eur. J.* **2004**, *10*, 831.
(31) Belanger, S.; Hupp, J. T. *Angew. Chem., Int. Ed.* **1999**, *38*, 2222.
(32) Schwab, A. D.; Smith, D. E.; Bond-Watts, B.; Johnston, D. E.; Hone, J.; Johnson, A. T.; de Paula, J. C.; Smith, W. F. *Nano Lett.* **2004**, *4*, 1261.

10.1021/ja0553912 CCC: $30.25

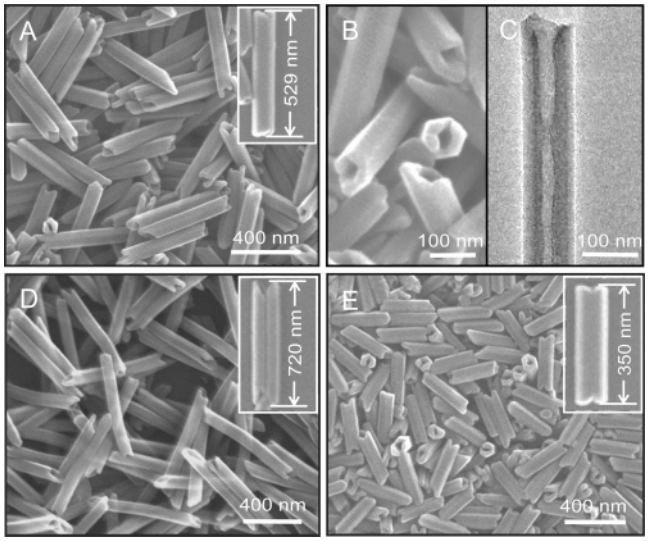

Figure 1. Low (A) and high (B) magnification SEM images and HRTEM image (C) of Sample I. SEM images of Sample II (D) and Sample III (E). The insets show the average longitudinal and lateral dimensions of the corresponding samples.

research of porphyrin on structural construction and utilization. Therefore, fabricating assembly with special and controllable structure is still a challenge in porphyrin study. Establishing an effective method to prepare desirable organic 1D nanostructures and to eventually convert them into a designed architecture is an increasing interest in chemistry and nanotechnology.

Here, we report the molecular self-assemblies of zinc meso-tetra (4-pyridyl) porphyrin (ZnTPyP). With the assistance of surfactant, a supramolecular self-assembly, hollow hexagonal nanoprism of ZnTPyP can be easily constructed with a tunable length and aspect ratio. The structural feature of the nanoprisms was characterized by transmission electron microscopy (TEM) and scanning electron microscopy (SEM). Furthermore, the one-dimensional (1D) assembly can self-organize into a three-dimensional (3D) superstructure through the simple evaporation of the solvent. The method is facile and efficient. The UV−vis adsorption and fluorescence spectra are employed to describe and reveal the growth process and photochemical property of the special self-assemblies. The internal structure of the hollow hexagonal nanoprism was investigated by X-ray diffraction (XRD).

Results and Discussion

When a stock solution of ZnTPyP/DMF (400 μL, 0.25 mM) was injected into 5 mL of continuously stirred aqueous CTAB (cetyltrimethylammonium bromide) solution in different concentrations at room temperature, the self-assembly of porphyrin molecules was formed. Figure 1 shows the results observed from a series of samples. Figure 1A is a typical SEM image of Sample I. For the preparation of Sample I, the concentration of CTAB was 0.4 mM. From this image, it can be seen that the sample is composed of a large amount of molecular rods with uniform size and shape as well as a smooth outside wall and an uneven terminal surface. The average length of a rod is ca. 530 nm as indicated in the inset of Figure 1A. In a high-magnification SEM image in Figure 1B from Sample I, it is evident that these rods possess an open and hexagonal end. The high-resolution TEM image in Figure 1C shows a strong contrast between the dark wall and the whitish center of the assembly, which is a typical feature of a hollow structure. The average thickness of the wall is about 30 nm. From the SEM and TEM observation, this structure can be called hollow hexagonal nanoprisms (HHNPs). In an energy-dispersed X-ray (EDX) analysis of the HHNPs, the elements of C, N, and Zn that constitute the molecules of ZnTPyP are clearly identified (see Figure S1 in Supporting Information), which confirms that the product is made from ZnTPyP. A statistical analysis is conducted by measuring over 200 HHNPs in TEM images. The results in Figure 2 show the dimensional distribution of the HHNPs in Sample I. It can be seen from the statistical results that the HHNPs are uniform in both lateral and longitudinal dimensions, giving an average length and outside diameter 529 $\pm$ 12 nm and 95 $\pm$ 3 nm, respectively.

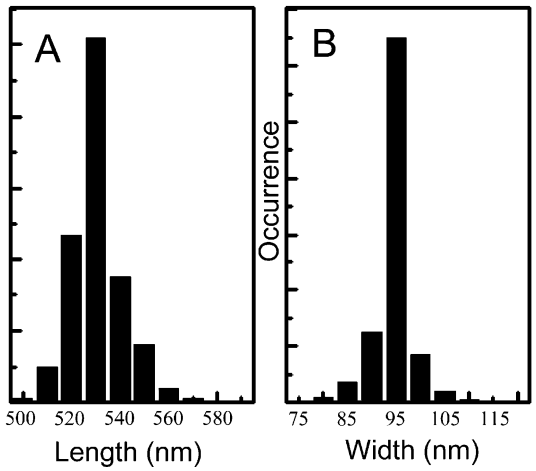

Figure 2. Distributions of the length and the width of HHNPs in Sample I.

The size and aspect ratio (i.e., longitudinal/lateral dimension) of the so-prepared self-assembled HHNPs can be tunable by changing the stoichiometric ratio of ZnTPyP over the surfactant CTAB. For example, Samples I, II, and III were prepared with the same concentration of ZnTPyP/DMF solution at 0.25 mM, while the concentrations of CTAB varied at 0.4, 0.2, and 0.8 mM, respectively. These changes result in the differences in the length and aspect ratio of the HHNPs as 530 $\pm$ 12 nm and 5.6 for Sample I, 720 $\pm$ 15 nm and 8.0 for Sample II, and 340 $\pm$ 10 nm and 3.5 for Sample III. The typical SEM images for the three samples are shown in Figure 1A, 1D, and 1E, respectively. The insets in these figures reveal the average length of HHNPs in each sample. It can be seen from the images that the length of the self-assembled HHNPs becomes shorter with the increase of the concentration of CTAB. When the concentration of CTAB was 0.8 mM, the length of HHNPs was ca. 350 nm, and when the concentration of CTAB was 0.2 mM, the length was 720 nm. On the other hand, when the concentration of ZnTPyP/DMF decreases from 0.25 mM to 0.06 mM, at the same concentration of CTAB at 0.4 mM as Sample I, the sizes of self-assemblies vary correspondingly from 95 nm $\times$ 529 nm to 34 nm $\times$ 200 nm (see Supporting Information Figure S2). The results indicate the effect of surfactant of CTAB on the formation and structure of HHNPs.

(33) Wang, Z.; Medforth, C. J.; Shelnutt, J. A. *J. Am. Chem. Soc.* **2004**, *126*, 15954.
(34) Wang, Z.; Medforth, C. J.; Shelnutt, J. A. *J. Am. Chem. Soc.* **2004**, *126*, 16720.

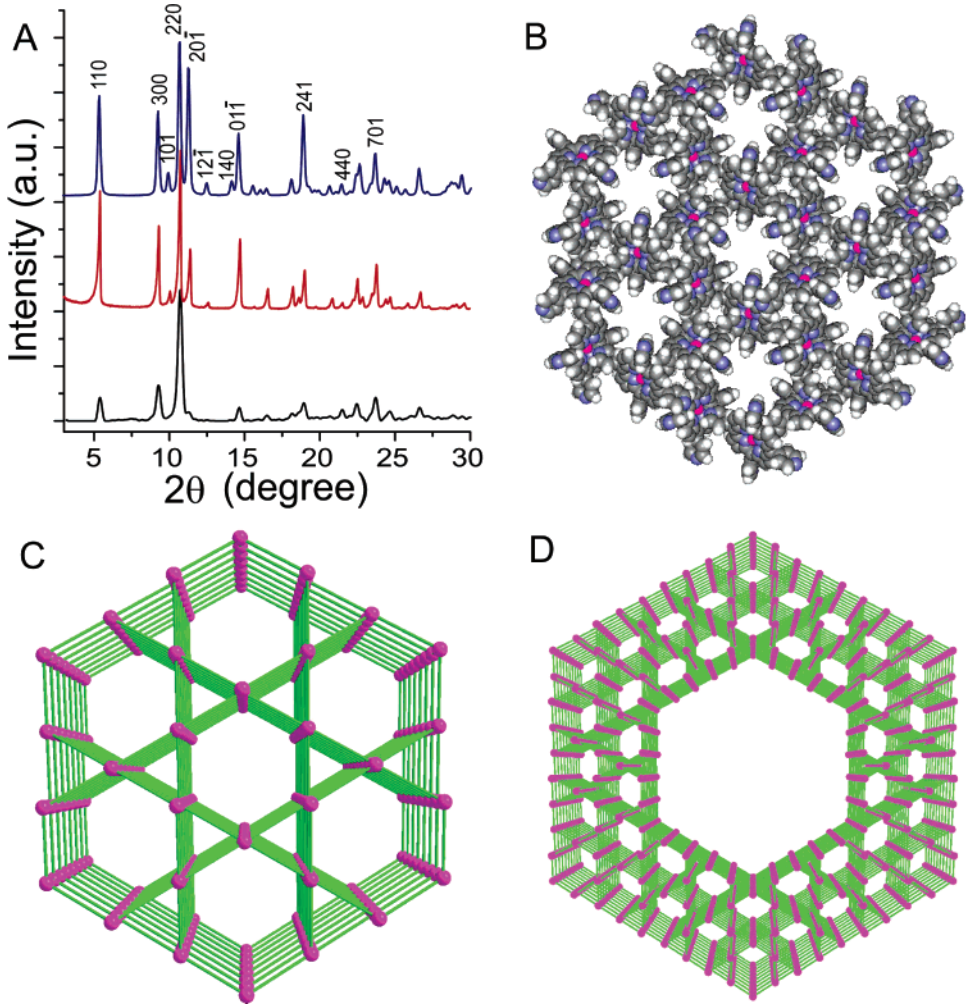

Figure 3. (A) XRD patterns of self-assembled porphyrin HHNP (black), porphyrin starting materials (red), and simulated pattern (blue) from the published crystal structure data (CCDC, Refcode YOVTOS). (B) Space-filling representation of an open-framework structure of HHNP along the crystallographic *c* axis. H_2O molecules are omitted for clarity. Zn, purple; N, blue; C, gray; H, white. (C) Perspective view of skeletal representation (Zn···Zn connections). (D) Perspective view of illustrative structure of self-assembled porphyrin HHNP. The illustrations are not drawn to scale.

The internal structure of the self-assembled porphyrin HHNP is investigated by XRD analysis. Figure 3 is the XRD patterns and the proposed structural models. In Figure 3A, the XRD pattern in black line is obtained from the self-assembled porphyrin HHNPs of Sample I, and the pattern in red line is from ZnTPyP bulk starting material of a commercial chemical. All of the peaks in the black pattern can be designated from the red pattern, which confirms that the nanoprisms consist of pure ZnTPyP. However, in the present experiment, the starting ZnTPyP molecules are self-assembled into a well-defined 1D nanostructure. To further ascertain the crystal structure and molecular self-assembly mode, we have searched the published crystal structures of zinc meso-tetra (4-pyridyl) porphyrin including its solvent clathrates and have theoretically simulated the XRD pattern as shown in Figure 3A in blue line. It can be found that all of the peaks in the XRD pattern of self-assembled HHNPs in black line can be indexed well according to the simulated pattern in blue line from the crystal structure obtained by Goldberg et al. (CCDC Refcode: YOVTOS).[35] The XRD pattern of HHNPs is significantly different from ones simulated from the reported crystal structures other than the above crystal structure. Therefore, it can be concluded that the HHNP has the same crystal structure with the crystal structure described by Goldberg et al. Specifically, porphyrin HHNP has a rhombohedral space group *R*3 with the unit cell dimensions $a = 33.145$ Å, $b = 33.145$ Å, $c = 9.374$ Å, $\alpha = \beta = 90°$, and $\gamma = 120°$. Figure 3B is a schematic illustration of a layer of HHNP along its *c* axis from the XRD results. In this model, the zinc atom at the center of ZnTPyP is six-coordinated to four pyrrole nitrogens of porphyrin core and to two pyridyl N-atoms of other porphyrins approaching from both side of the molecular framework.[35] Each porphyrin monomer is thus strongly linked to four neighboring porphyrin units. The structure can be also described as one consisting of a circular hexametric cage cross-linked by axial coordination of pyridyl ligands, which propagates in three different directions of the trigonal lattice. A notable feature of such a structure is that the center of the hexametric cage has a large cavity about 19 Å with a functional pyridine window where water molecules may be ligated through hydrogen bondings.[35,36] The adjacent circular hexametric cage arrays interpenetrate each other in the crystal structure and are "glued" by noncovalent $\pi-\pi$ interactions between porphyrin molecules, which may be further stabilized by water species bridges.[36] This

(35) Krupitsky, H.; Stein, Z.; Goldberg, I.; Strouse, C. E. *J. Inclusion Phenom.* **1994**, *18*, 177.

(36) Lin, K.-J. *Angew. Chem., Int. Ed.* **1999**, *38*, 2730.

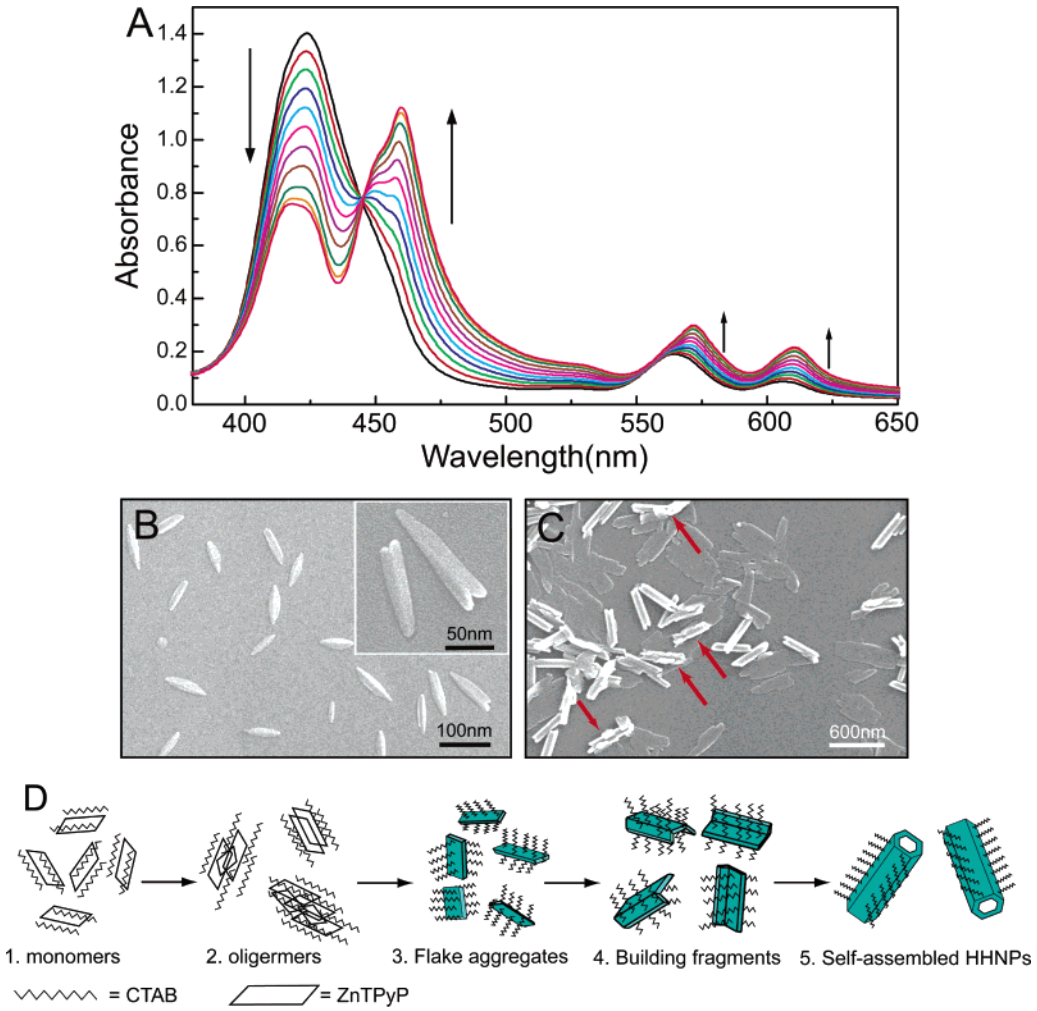

Figure 4. (A) UV−vis spectra obtained at every 30 s from the beginning of stock solution injection. There is an isosbestic point corresponding to J-aggregates. SEM images acquired at 150 s (B) and 240 s (C) after injection. The inset in B shows the enlarged angular flakes. The red arrows in C indicate the fragments of incomplete self-assembled structures. (D) Schematic illustration of the formation process of HHNPs (not to scale).

structure results in a hexagonal channel with the dimension of $a/2 \times a/\sqrt{3}$ (16.6 Å × 19.1 Å) along the crystallographic *c* axis, as shown in Figure 3C.

In the XRD patterns of Figure 3A, it can be further observed that the relative intensity of the characteristic (220) and (440) peaks in HHNPs (black pattern) remarkably increases compared to those in the ZnTPyP starting material and simulated pattern. Moreover, the (101) peak in HHNP XRD pattern vanishes and the intensities of the peaks of $(01\bar{1})$ and $(20\bar{1})$ decrease significantly. These features indicate that ZnTPyP molecules in HHNPs prefer to self-assemble and to grow along the crystallographic *c* axis. That is, the longitudinal direction of HHNP is the crystallographic *c* axis, which reveals that the wall of HHNP possesses heaps of the hexagonal channels parallel to the *c* axis as shown in Figure 3D.

The UV−vis spectrum and SEM image are used to monitor the formation process of ZnTPyP HHNP. Figure 4A shows the successive UV−vis spectra acquired at every 30 s in the self-assembled process of Sample I. It can be seen that the low-energy Soret band at 460 nm, associated with J type aggregate mode,[37,38] increases gradually while the high-energy Soret band at 424 nm, associated with monomer, decreases gradually. From about 360 s onward, the spectra remain unchanged, indicating that the aggregation process reaches a steady state. The rapid evolution of the UV−vis spectra demonstrates a fast nucleation process followed by facile growth. The SEM images in Figure 4B and 4C are acquired at two different time periods in the course of the self-assembly of Sample I, showing the corresponding intermediate morphologies of the HHNPs. As shown in Figure 4B, some angular objects begin to appear at about 150 s after the reaction starts where the intermediates are fairly short with sharp ends. At about 240 s of the reaction, the assembly further proceeds where the coexistence of HHNP and incomplete structures is visible (Figure 4C).

On the basis of the above experimental results, we propose a tentative mechanism to illustrate the formation process of ZnTPyP HHNP as shown in Figure 4D. Initially, ZnTPyP monomers and CTAB surfactant molecules start to self-assemble and form porphyrin/surfactant complex under the hydrophobic interaction between the alkyl chains of CTAB and porphyrin molecules.[37,39,40] With the diffusion of DMF into water, por-

(37) Maiti, N. C.; Mazumdar, S.; Periasamy, N. *J. Phys. Chem. B* **1998**, *102*, 1528.
(38) Okada, S.; Segawa, H. *J. Am. Chem. Soc.* **2003**, *125*, 2792.
(39) Barber, D. C.; Freitag-Beeston, R. A.; Whitten, D. G. *J. Phys. Chem.* **1991**, *95*, 4074.
(40) Lucia, L. A.; Yui, T.; Sasai, R.; Takagi, S.; Takagi, K.; Yoshida, H.; Whitten, D. G.; Inoue, H. *J. Phys. Chem. B* **2003**, *107*, 3789.

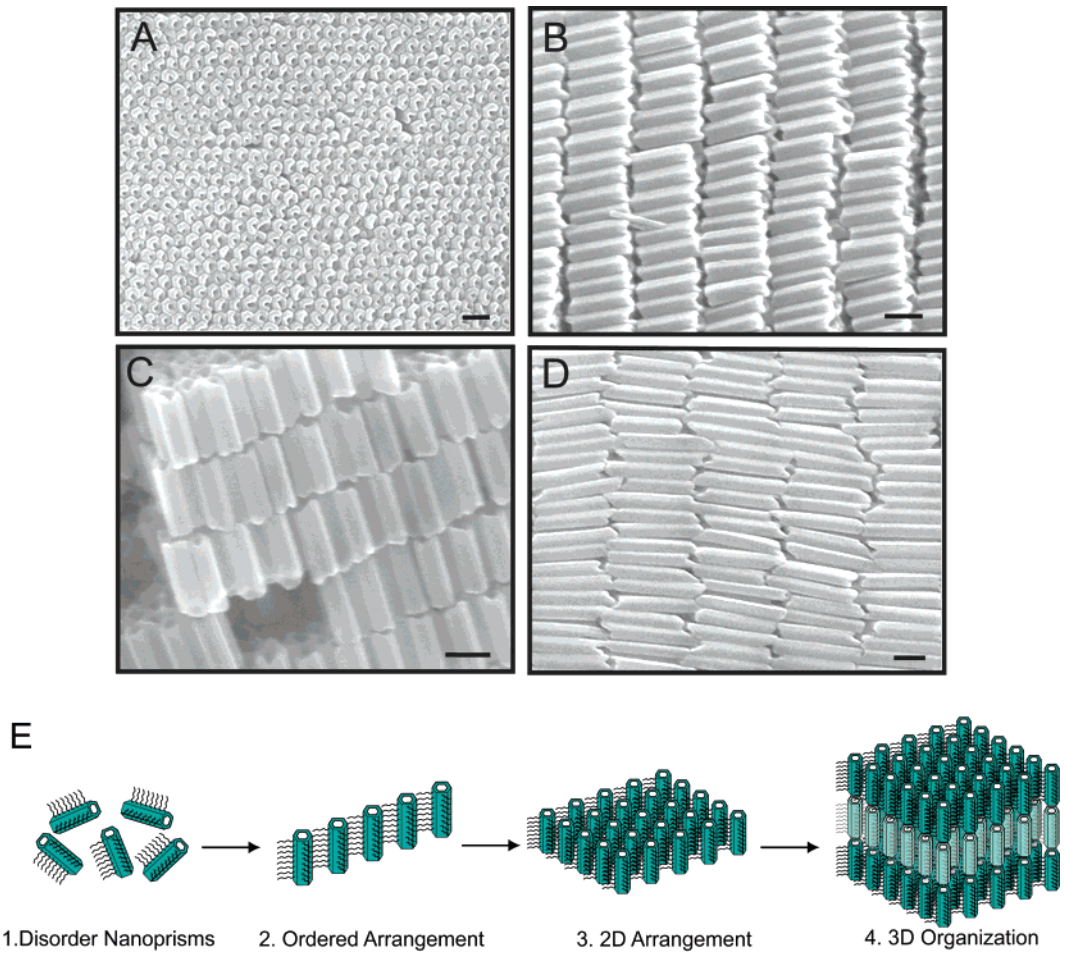

Figure 5. SEM images of 3D smectic superstructures self-organized by HHNPs. A smectic layer of Sample III in vertical alignment (A), horizontal alignment (B), and horizontal alignment with defects showing a layer-by-layer structure (C). (D) Top view of Sample I in horizontal alignment. The bar length is 200 nm. (E) A schematic illustration of the possible self-organization process of HHNP assemblies.

phyrin molecules form dimers, and the dimers aggregate with surfactant molecules. The Zn−N axial coordination of pyridyl N-atoms to zinc atoms of ZnTPyP molecules promotes the growth of aggregates, which continue to grow into a flake structure mainly driven by crystal packing force and $\pi-\pi$ stacking interaction among adjacent ZnTPyP molecules. The difference of the metal ligation and strong $\pi-\pi$ stacking interactions in the three dimensions leads to the different growth rates that eventually result in the formation of a HHNP. The hexagonal shape and preferred growth along the *c* axis of the HHNP are dependent on the specific intermolecular reaction and crystal packing force among ZnTPyP molecules.[38] In a control experiment (not shown here), we find the Zn−N axial coordination is important to form these one-dimension assemblies. When zinc *meso*-tetra (4-phenyl) porphyrin (ZnTPP) or *meso*-tetra (4-pyridyl) porphyrin (TPyP) was used as the starting material instead of ZnTPyP, defined one-dimensional self-assembled structures cannot be obtained. On the other hand, although the exact step-by-step kinetics of the HHNP formation is not yet known, it is evident that the presence of CTAB surfactant molecules plays an important role in the self-assembled process.[40,41] The influence of surfactants or other additives on crystal morphologies has been well reported in earlier research.[42,43] In the present experiment, the irregular rods were found in the absence of surfactant (see Figure S3 in Supporting Information). However, the schematic illustration in Figure 4D is only a temporary and possible description of the HHNP formation. The role of surfactant in the nanostructure formation should be investigated in detail.

In analogy to biological systems, molecular self-assembled primary structures need to further be organized into secondary, tertiary, or quaternary levels of superstructures, which are very important to many of the devices based on organic or hybrid inorganic−organic compounds.[16−22] It has been reported that some inorganic building blocks can be organized into a higher order ensemble with advanced function, such as photonic band gap crystal,[44] whereas few examples are available for an organic system.[16,17] In the present study, it is found that the molecularly self-assembled HHNPs can organize into 3D smectic superstructures after the evaporation of the solvent. For this purpose, droplets of concentrated HHNP aqueous solution are deposited on silicon substrate. After the evaporation of water, the remains are examined by using SEM. Figure 5A is a typical SEM image of the superstructures with Sample III in vertical alignment, showing that the self-organized HHNPs are in a hexagonal close-packed architecture with a core-to-core distance of about 100

(41) Balaban, T. S.; Leitich, J.; Holzwarth, A. R.; Schaffner, K. *J. Phys. Chem. B* **2000**, *104*, 1362.
(42) Berkovitch-Yellin, Z.; van Mil, J.; Addadi, L.; Idelson, M.; Lahav, M.; Leiserowitz, L. *J. Am. Chem. Soc.* **1985**, *107*, 3111.
(43) Weissbuch, I.; Zbaida, L.; Leiserowitz, L.; Lahav, M. *J. Am. Chem. Soc.* **1987**, *109*, 1869.
(44) López, C. *Adv. Mater.* **2003**, *15*, 1679.

nm between adjacent HHNPs. Figure 5B is an SEM image in horizontal alignment. The images exhibit a highly ordered 3D self-organized architecture with remarkable smectic characteristics, composed of a large number of HHNPs as building blocks. Figure 5C is an SEM image with defects in horizontal alignment. In this image, it is clear that the ZnTPyP HHNPs have self-organized into a well-ordered lattice with a layer-by-layer structure. This densely packed architecture can form a domain of tens to hundreds of square micrometers with the possibility of extending further over an even larger area. Thus, we believe that the self-assembled porphyrin HHNPs can be used potentially as nonspherical building blocks for many fields such as optical nanodevices, biomaterials filter, and photonic band gap crystal as a result of their remarkable monodispersity and simple preparation in large scale. Moreover, other samples such as Sample I can also self-organize into the 3D architecture as shown in Figure 5D.

A schematic illustration for the organization process of HHNPs is proposed in Figure 5E. The presence of surfactant is also considered to be important in the 3D self-organization of the porphyrin HHNPs. The hydrophobic interactions among alkyl chains of CTAB on the external surface of HHNPs and among adjacent HHNPs are the key driving force for the self-organization. Such driving force is also proposed for a mesoscale assembly of surfactant-coated nanoparticles with high shape anisotropy.[22] Analogous to the monodispersed inorganic building blocks such as quantum dots, rods, and wires,[45,46] it is likely that the smooth external side surface, the uniform hexagonal external geometry, and the good monodispersity exert important effects on regulating the spontaneous formation of a well-ordered 3D superlattice. The hydrophobic driving force that is strengthened by collective intermolecular couplings in the architecture is responsible for the transitions from random to ordered mesophase associated with the pendant surfactant molecules that function over an elongated scale to produce the giant three-dimensional organization.

Conclusion

In summary, this study has successfully developed an effective and facile method for self-assembling porphyrin molecules into hollow hexagonal nanoprisms with uniform size and shape and controllable aspect ratio. The controlled experiments allow one to tailor the size and aspect ratios of the porphyrin nanoprisms. The XRD study reveals that the hollow nanoprisms have the trigonal structure with the space group *R*3 and prefer to grow along the crystallographic *c* axis. Furthermore, the self-assembled porphyrin HHNPs can easily self-organize into the well-ordered 3D smectic superstructures through simple evaporation of the used solvent as a result of the good monodispersity and regular geometric shape. The finding extends the surfactant-assisted self-organization from the inorganic system to the organic system of porphyrin. Owing to the rich catalytic, photochemical, electrochemical, and biochemical activities, the 1D hexagonal hollow prisms and their 3D architectures are expected to be useful in the application of porphyrin in diverse fields.

(45) Peng, X. G.; Manna, L.; Yang, W. D.; Wickham, J.; Scher, E.; Kadavanich, A.; Alivisatos, A. P. *Nature* **2000**, *404*, 59.
(46) Nikoobakht, B.; Wang, Z. L.; El-Sayed, M. A. *J. Phys. Chem. B* **2000**, *104*, 8635.

Scheme 1. Molecular Structure of ZnTPyP

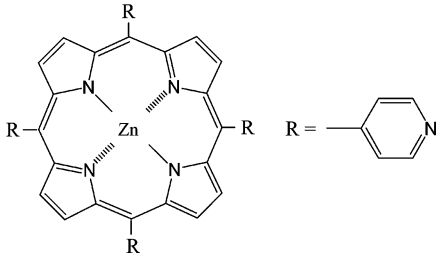

Experimental Section

Materials. The compounds of zinc meso-tetra (4-pyridyl) porphyrin (ZnTPyP, Scheme 1) and cetyltrimethylammonium bromide (CTAB) used in this study were purchased from Aldrich Chemical Co. *N*,*N*-dimethylformamide (DMF) (A. R.) was used as the solvent of ZnTPyP and was purchased from Beijing Chemical Reagent Corp., China. Ultrapure water with a resistivity $\geq$18.2 MΩ cm was produced using a Milli-Q apparatus (Millipore) and was filtered using an inorganic membrane with a pore size of 0.02 μm (Whatman International, Ltd.) just before use.

Sample Preparation Methods. The nanoprisms of zinc meso-tetra (4-pyridyl) porphyrin were synthesized through a simple solution procedure. In a typical preparation, 400 μL of stock ZnTPyP and DMF solution (0.25 mM) was injected into 5 mL of continuously stirred aqueous solution of CTAB with different concentrations at room temperature (25 °C). Then, the mixture was stirred for 10 min. The resulting solution became greenish transparent colloidlike solution without precipitation for several months. In this study, three samples with the concentration of CTAB (C_{CTAB}) = 0.4, 0.2, and 0.8 mM were prepared and were assigned as sample I, II, and III, respectively. Ultrapure water was used in all experiments.

For electron microscopy observation, the products were centrifuged at 9000 rpm and were washed twice with Millipore water to remove the surfactant deposited onto silicon wafer substrate and copper grid for the characterization of scanning electron microscopy and transmission electron microscopy, respectively. A Hitachi S-4300F scanning electron microscope equipped with energy-dispersive X-ray analyzer (Phoenix) was used to investigate the morphology of the hollow hexagonal nanoprisms of ZnTPyP. TEM images were collected by using a JEM JEOL 2010 operated at 200 kV. X-ray diffraction measurement was carried out with a Rigaku D/max-2500 using filtered Cu Kα radiation. UV−vis spectroscopy (UV-1601PC, SHIMADZU) was used to characterize the optical absorbance of the porphyrin nanoprisms. Photoluminescence (PL) spectra were measured in a HITACHI F-4500 Fluorescence Spectrophotometer at room temperature. The excitation wavelength is 422 nm.

Acknowledgment. The authors thank Prof. C. L. Bai, Prof. Z. G. Shuai at Institute of Chemistry, Chinese Academy of Sciences, Prof. Z. L. Wang at Georgia Institute of Technology, and Prof. F. Huang at Fujian Institute of Research on the Structure of Matter, Chinese Academy of Sciences, for discussion. This work is partly supported by National Natural Science Foundation of China (Grant Nos. 20025308, 20520140277, and 20575070), National Key Project on Basic Research (Grant Nos. G2000077501 and 2002CCA03100), and the Chinese Academy of Sciences.

Supporting Information Available: The low-magnification SEM and TEM images of porphyrin HHNPs, EDX, UV−vis, and FL spetra. Complete ref 14 is provided. These materials are available free of charge via the Internet at http://pubs.acs.org.

JA0553912